Available online at www.sciencedirect.com
ScienceDirect
Journal of the European Ceramic Society 31 (2011) 893–901
www.elsevier.com/locate/jeurceramsoc

Mechanical properties of sintered ZrB_2–SiC ceramics

Shi C. Zhang *, Greg E. Hilmas, William G. Fahrenholtz

Department of Material Science and Engineering, Missouri University of Science and Technology, 222 McNutt Hall, 1870 Miner Circle, Rolla, MO 65401, United States

Received 25 June 2010; received in revised form 4 November 2010; accepted 21 November 2010
Available online 28 December 2010

Abstract

ZrB_2 ceramics containing 10–30 vol% SiC were pressurelessly sintered to near full density (relative density >97%). The effects of carbon content, SiC volume fraction and SiC starting particle size on the mechanical properties were evaluated. Microstructure analysis indicated that higher levels of carbon additions (10 wt% based on SiC content) resulted in excess carbon at the grain boundaries, which decreased flexure strength. Elastic modulus, hardness, flexure strength and fracture toughness values all increased with increasing SiC content for compositions with 5 wt% carbon. Reducing the size of the starting SiC particles decreased the ZrB_2 grain size and changed the morphology of the final SiC grains from equiaxed to whisker-like, also affecting the flexure strength. The ceramics prepared from middle starting powder with an equiaxed SiC grain morphology had the highest flexure strength (600 MPa) compared with ceramics prepared from finer or coarser SiC powders.

Keywords: Zirconium diboride; Silicon carbide; Particle size; Mechanical properties

1. Introduction

ZrB_2 is one of the ultra-high temperature ceramics (UHTCs). These compounds are typically early transition metal borides and carbides,[1,2] such as ZrB_2, HfB_2, TaC and ZrC. The ultra-high melting temperatures (>3000 °C) of UHTCs make them candidates for applications that require exposure to extreme thermal and chemical environments such as those associated with atmospheric re-entry, hypersonic flight, and rocket propulsion.[3–5] However, oxidation of refractory diborides in air at elevated temperatures has limited their applications.[5–7] One of the commonest additives used to improve the oxidation protection of ZrB_2 and HfB_2 is silicon carbide (SiC),[6,8,9] in the range of 10–30 vol% SiC, which forms coherent layers of SiO_2-based glasses on the surface of the ceramics. This continuous scale provides passive oxidation protection through the intermediate temperature regime (∼1100–1600 °C or higher). Therefore, the ZrB_2–SiC ceramics have received great attention in the last decade.[10–20]

In addition to improving the oxidation behavior, the introduction of SiC particles into ZrB_2 ceramics offers the additional benefit of improving the mechanical properties of ZrB_2 ceramics.[21–24] Chamberlain et al.[21] reported that the addition of SiC particles into ZrB_2 increased the fracture strength of hot-pressed ZrB_2 ceramics from ∼560 MPa for monolithic to over 1000 MPa for SiC contents of 20 or 30 vol%. Monteverde[23] also reported that the fracture strength of hot-pressed ZrB_2 increased from 350 MPa for monolithic ZrB_2 to 835 MPa when 30 vol% of fine SiC was added.

Because ZrB_2 and SiC have strong covalent bonding and low self-diffusion coefficients, ZrB_2 ceramics with SiC additions have typically been densified by hot pressing.[5,21,22] or reaction hot-pressing.[25] The relatively simple shapes (e.g., right regular cylinders) that are produced by hot-pressing must then be machined to the final desired geometries using expensive diamond machining techniques. Recent studies have shown that ZrB_2–SiC can achieve near theoretical density by pressureless sintering, eliminating one of the barriers to more widespread use of these high strength, high hardness ceramics.[26,27]

Pressureless sintered ZrB_2–30 vol% SiC ceramics, reported in a previous study,[26] have comparable elastic modulus, hardness and fracture toughness to hot pressed ZrB_2–SiC materials.[3] However, ZrB_2–SiC produced by pressureless sintering had a lower strength of 460 MPa,[26] compared to typical values of strength in the range of 600–800 MPa[21,25,28,29] for ZrB_2–SiC densified by hot pressing. The recent studies by Zhu et al.[30]

* Corresponding author.
E-mail address: scz@mst.edu (S.C. Zhang).

0955-2219/$ – see front matter © 2010 Elsevier Ltd. All rights reserved.
doi:10.1016/j.jeurceramsoc.2010.11.013

Table 1
Characteristics of the starting raw materials.

Material	Phases	Grade	Mean particle size (μm)	Surface area (m^2/g)	Oxygen (wt%)	Supplier
ZrB_2	Hexagonal	B	2	1	0.9	H.C. Starck
ZrB_2	Hexagonal	B	0.6	1.6	1.9	Attrition Milled
SiC	α-phase	UF-5	1.45	∼5	–	H.C. Starck
SiC	α -phase	UF-10	1.05	10	–	H.C. Starck
SiC	α -phase	UF-25	0.45	25	2.0	H.C. Starck
B_4C	Hexagonal	HS	0.25	15.8	1.3	H.C. Starck
Resin	40wt% C	–	–	–	–	Georgia Pacific

have shown that the flexure strength of hot pressed ZrB_2–SiC materials is controlled by the SiC grain size. When the average SiC grain size in hot pressed ZrB_2–SiC was ∼6 μm, the flexure strength was less than 400 MPa. Strengths over 900 MPa have only been reported for materials with SiC particle sizes of 1 μm or less. In the previous study,[26] whisker-like SiC grains with ∼20 μm length were observed in pressureless sintered ZrB_2–SiC ceramics when fine SiC starting powder (average particle size ∼0.45 μm) was used. Therefore, the finer SiC powder resulted in SiC grains with an elongated morphology after sintering, in contrast to the equiaxed SiC grains observed by Monteverde[23] in hot-pressed ZrB_2–SiC composites when the same raw SiC powder was used. The elongated SiC grains appear to decrease the flexure strength of sintered ZrB_2–SiC ceramics.

The present research focuses on the effects of the SiC starting particle size on the final ZrB_2 grain size, as well as dispersed SiC particle size and morphology, for sintered ZrB_2-based ceramics containing 10, 20, and 30 vol% SiC. Mechanical properties, such as elastic modulus, hardness, flexure strength and fracture toughness were evaluated to understand the role of SiC content and SiC particle morphology on mechanical behavior.

2. Experimental procedure

2.1. Powder preparation and characterization

Zirconium diboride (Grade B, ∼2 μm particle size, H.C. Starck, Karlsruhe, Germany) and three SiC powders with different starting particle sizes (UF-5 with a particle size of 1.45 μm, UF-10 with a particle size of 1.05 μm, and UF-25 with a particle size of 0.45 μm, H.C. Starck) were the starting materials used in the present study. To reduce the particle size, the as-received ZrB_2 was attrition milled for 2 h using WC media and either hexane or methylethyl ketone (MEK) as the solvent. During milling, a flowing argon gas atmosphere was maintained around the milling bucket to minimize oxidation of the ZrB_2 powder during the milling process. The amount of WC picked up by the powder during milling was calculated based on the milling media weight loss after milling. A soluble phenolic resin (GP 2074, Georgia Pacific Co., Atlanta, GA) was added as a carbon precursor. The particle sizes were measured by laser light scattering (LS230 Particle Size Analyzer, Beckman Coulter, Fullerton, CA). The specific surface areas were measured by nitrogen adsorption (NOVA 1000, Quantachrome, Boynton Beach, FL). The phase compositions were determined by X-ray diffraction (XDS 2000, Scintag Inc., USA). The oxygen contents were measured using a Leco Furnace method (performed by NSL Analytical Services, Cleveland, OH). The major crystalline phase, grade, specific surface area, oxygen content, and supplier are listed for each powder in Table 1.

2.2. Specimen preparation

In a previous study,[26] it was confirmed that the oxide impurities on ZrB_2 and SiC particle surfaces caused grain coarsening below the optimum solid-state sintering temperatures, which inhibited densification. Further, B_4C and carbon were effective sintering additives for ZrB_2 because they reacted with and removed the surface oxides, which allowed for pressureless densification of ZrB_2–SiC ceramics. Because the homogeneity of both the SiC and the sintering additive (B_4C) will affect the densification behavior and final microstructure of the resultant ceramics, batches were mixed in MEK or xylene by ball milling with a dispersant (BYK 110, BYK Chemie Co., Willingford, CT) using WC media. The optimum dispersant concentrations for the three powders were determined using settling experiments. To produce bars for the mechanical properties study, slurries of ZrB_2 with SiC (10, 20, or 30 vol%) and B_4C (4 wt% based on the weight of ZrB_2) were ball milled at a rate of 60 rpm for 24 h using WC beads as milling media and MEK as a solvent. The weight ratio of WC media to powders was about 1:1. The optimum concentrations of the surfactant, BYK 110, for ZrB_2, SiC and B_4C were 0.1 1.0 and 5.0 mg of surfactant per gram of powder, respectively. After ball milling, 1 wt% binder (Qpac-40 polypropylene carbonate) or phenolic resin (2.8 to 10.0 wt% of carbon based on the weight of SiC) was added and the mixture was milled for an additional 24 h. Due to the use of an inert solvent and a sealed plastic bottle, the change in oxygen content of ZrB_2 and SiC was considered to be negligible during the ball milling step. After milling, the slurry was dried in a beaker with constant stirring to prevent segregation of the components due to differential sedimentation. The dried powder cake was ground using an agate mortar and pestle and sieved (−50 mesh, ∼300 μm) to form granules for dry pressing. For the mechanical properties studies, 44.5 mm (1.75 in.) diameter disks were formed by uniaxial dry pressing at 19 MPa (2.7 ksi) followed by cold isostatic pressing (CIP) at 310 MPa (45 ksi). The green density of each disk was calculated using the mass of the disk and the volume calculated from the disk dimensions. The disks with carbon additions, using phenolic resin as the precursor, were charred at 600 °C for 2 h in a flowing 90Ar/10H_2 atmosphere to convert the resin to carbon. The disks were then stored in a

vacuum desiccator to minimize possible oxidation in air prior to sintering. Assuming added carbon was consumed by reaction with the silica (SiO_2) on the surface of the SiC particles, and the residual ZrO_2 on the surface of the ZrB_2 particles was removed by reaction with both the B_4C and the WC introduced by the attrition milling process (~3 wt% based on WC media loss due to wear), the theoretical densities for ZrB_2 with 10, 20 and 30 vol% SiC were calculated.

2.3. Densification

All of the disks were sintered using graphite crucibles in a resistance heated graphite element furnace (3060-FP20, Thermal Technology Inc., Santa Rosa, CA). Pressed disks were heated at 10 °C/min to 1450 °C. To facilitate removal of oxide impurities from the surfaces of ZrB_2 and SiC, the heating schedule included isothermal holds of 1 h at both 1250 °C and 1450 °C, followed by heating at 20 °C/min to temperatures ranging from 1850 °C to 2050 °C for densification. The furnace atmosphere was a mild vacuum (~20 Pa) at temperatures of 1650 °C or below and was switched to flowing argon (~10^5 Pa) for temperatures above 1650 °C. The disks were held at the specified sintering temperatures for 1–4 h. The bulk densities of sintered specimens were measured using Archimedes' method. Relative densities were calculated by dividing the measured bulk density by the appropriate, calculated theoretical density that was based on the nominal pellet composition. Some sintered specimens were surface ground, polished, and thermally etched at 1550–1750 °C for scanning electron microscopy (SEM; S-570 Hitachi, Japan) analysis. The grain size of SiC grains was quantified using image analysis software (Image J, National Institutes of Health, Washington D.C.) by counting at least 100 ZrB_2 or SiC grains.

2.4. Mechanical properties

The flexure strength at room temperature was measured in four-point bending according to ASTM C1161-02a for type A bars using a screw-driven test frame (Model 5881, Instron, Norwood, MA). The reported flexure strengths are the average of at least 10 specimens. The elastic moduli were measured according to ASTM Standard C1259-01 for impulse excitation of cylindrical discs (Grindosonic, J.W. Lemmens, St. Louis, MO). Vickers' hardness was determined from the average of at least ten indents produced using a 500 g load, with 15 s hold, on the surface of specimens polished to a 1 μm diamond finish. The fracture toughness was determined by the indentation flexure method according to ASTM Standard C1421.

3. Results and discussion

3.1. Effect of carbon content on the strength of ZrB_2–SiC

According to a previous study,[26] the stoichiometric amount of carbon required to remove the SiO_2 on the UF-25 SiC particle surfaces was determined to be 2.8% of the SiC weight in the batch, based on a measured oxygen content of 2.0 wt% for UF-25 SiC. Since some carbon may be consumed by reaction with B_2O_3 or ZrO_2, the actual carbon additions needed to be more than the stoichiometric amount. In the present study, batches were prepared with 2.8, 5, and 10 wt% carbon (based on SiC weight). The relative densities of the sintered materials are list in Table 2. As seen from the table, the sintered density of ZrB_2–30% SiC with 2.8 wt% carbon addition was only 96.7% even though it was sintered at 2000 °C for 3 h. In contrast, batches containing 5 and 10 wt% carbon could be sintered to near full density at lower temperatures (e.g., 99.1% after sintering at 1950 °C for 5 wt% carbon). This indicated that the stoichiometric carbon addition was not enough to facilitate complete densification of ZrB_2–SiC ceramics by pressureless sintering.

Table 2
Sintered density of ZrB_2–30% SiC with various carbon additions.

Carbon content based on SiC (UF-25) (wt%)		10%	5%	2.8%
T (°C)	t (h)			
1875	3	98		
1950	3		99.1	96.2
2000	3		99.5	96.7

Based on the densification results, two series of 44.5 mm diameter disks, containing 10, 20, or 30 vol% SiC with either 5 or 10 wt% carbon additions were prepared. These pellets were cut and ground to produce specimens for mechanical property measurements and microstructural studies. The average flexure strengths calculated from at least 10 specimens of all six compositions are plotted in Fig. 1. The 5 wt% carbon addition sintered at 1950 °C resulted in higher flexure strengths (400–490 MPa), compared with a 10% carbon addition sintered at 1875 °C (325–380 MPa). This result can be explained by observation of the differences in the microstructures for the different carbon contents, using ZrB_2–30%SiC as an example (Fig. 2). As shown in the pressureless sintering study of ZrB_2–SiC,[26] ZrB_2–30% SiC with 7.3% carbon appeared to have residual carbon at the ZrB_2/SiC grain boundaries, whereas the ZrB_2–30% SiC specimens with ≤5% carbon did not contain residual carbon within their microstructures. Further, the resid-

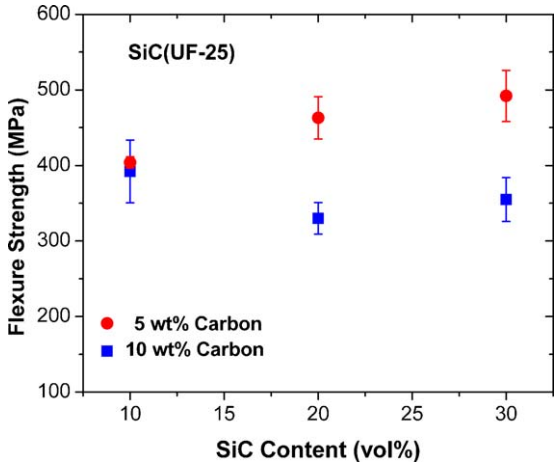

Fig. 1. Comparison of the flexure strength of ZrB_2–SiC ceramics with carbon additions of 5 and 10 wt% as a function of SiC content.

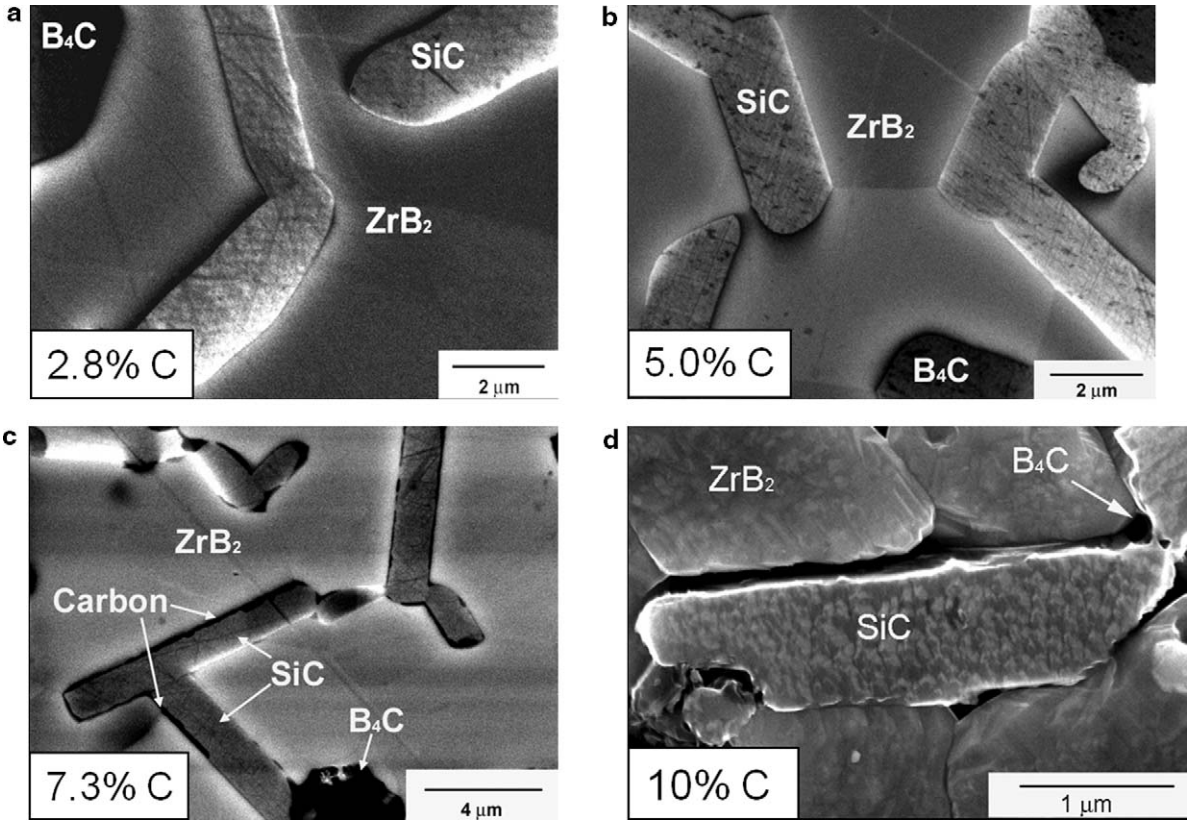

Fig. 2. SEM images of the microstructures of ZrB_2–30 vol% SiC with carbon additions of 2.8 wt% (A), 5.0 wt% (B), 7.3 wt% (C), and 10 wt% (D). In (C) and (D) excess carbon resulted in formation of residual carbon at the ZrB_2/SiC grain boundaries.

ual carbon in the ZrB_2–30% SiC specimen with 10 wt% carbon was more prevalent and was readily removed during polishing. It should be noted that ZrB_2–10 vol% SiC specimens with the different carbon additions had almost the same flexure strength, but the flexure strength of the ZrB_2–SiC specimens with carbon additions of 10 wt% were lower than specimens with a 5 wt% carbon addition for SiC contents of 20 and 30 vol%. The decrease in strength for the higher SiC content specimens was due the higher SiC content of these materials, which resulted in a larger volume fraction of excess carbon that deposited at the grain boundaries. The residual carbon at the grain boundaries is likely to act as the failure origin due to its low strength relative to the ceramic matrix. Since densification of ZrB_2–SiC materials with 2.8 wt% carbon additions was difficult, and carbon additions of 7.3 and 10 wt% had residual carbon and lower mechanical strengths, 5 wt% carbon was selected as the optimum addition for further studies.

3.2. Effect of SiC content on the strength of ZrB_2–SiC

To investigate the effect of SiC volume fraction on the mechanical properties of sintered ZrB_2–SiC materials, pellets for mechanical property tests were prepared with three different volume fractions of SiC (10, 20 and 30 vol%) and 5 wt% carbon based on the weight of SiC. The finest SiC (UF-25, particle size = 0.45 μm) was selected as the starting powder. The relative density of all of the ZrB_2–SiC samples sintered at 2000 °C in Ar for 3 h was >97% of theoretical (as shown in Table 3). The average flexure strength of ZrB_2 containing 10, 20 and 30 vol% UF-25 SiC and 5 wt% carbon additions were 404, 463 and 492 MPa, respectively. Other mechanical properties were analyzed and the results are summarized in Table 3. As seen from the table, the elastic modulus, hardness and flexure strength of ZrB_2–SiC materials all had the same trend, i.e., the values of the properties increased with increasing SiC volume fraction. The elastic moduli reported for ZrB_2 are in the range of 520–550 GPa[31] while the value for α-SiC is reported to be 415 GPa.[32] Therefore, the elastic moduli of ZrB_2–SiC composites should decrease with increasing SiC fraction based on a volumetric rule of mixtures calculation. The results contradict the rule-of-mixtures calculation. Therefore, microstructural analysis of the three materials was performed to determine the dependence of the mechanical properties on the resultant microstructures.

Fig. 3 compares the microstructures of ZrB_2 containing 10, 20 and 30 vol% UF-25 SiC and 5 wt% C. Microstructural analysis revealed that the SiC grains in all three compositions had a predominantly whisker-like morphology. The aspect ratios of the elongated SiC grains for each material were statistically evaluated using 100 SiC grains from each composition. The aspect ratios of the elongated SiC grains in the pressureless sintered ZrB_2–SiC materials are almost the same, at approximately 4. Based on this analysis, it appears that 10 vol% SiC (0.45 μm particle size) is already above the percolation threshold for the

Table 3
Comparison of mechanical properties of ZrB_2 with 10, 20, and 30 vol% SiC.

SiC volume fraction (vol%)	10	20	30
Carbon addition (wt%)	5% Based on the SiC weight		
B_4C addition (wt%)	4% Based on ZrB_2 weight		
Sintering conditions	2000 °C/3 h	2000 °C/3 h	2000 °C/3 h
Sintered density (%)	~97	>97	>99
Elastic modulus (GPa)	446 ± 7	474 ± 7	490 ± 7
Hardness (GPa)	15.3 ± 1.2	18.8 ± 1.1	22.4 ± 0.7
Flexure strength (MPa)	404 ± 62	463 ± 53	492 ± 49
Toughness (MPa $m^{1/2}$)	3.1 ± 0.1	3.4 ± 0.1	3.5 ± 0.3

SiC particles in the ZrB_2 matrix, which means that the SiC particles can coarsen because they are in contact during sintering, as discussed in the previous study.[26] Because all of the ceramics contain SiC with the same aspect ratio, the morphology of the SiC grains should have no effect on mechanical properties of ZrB_2–SiC ceramics using the same SiC powder.

The average ZrB_2 and SiC grain sizes for each composition, again using an average of at least 100 grains, are plotted in Fig. 4. As seen from the graph, the ZrB_2 grain size decreased from ~5 μm for a SiC content of 10 vol% down to ~2 μm for a SiC content of 30 vol%. Based on this observation, ZrB_2 grain growth appears to be inhibited, or pinned, by the dispersed SiC particles. In addition, to the ZrB_2 grain size, the average SiC grain size was also evaluated using a computed average of the length and width of each elongated SiC grain. Based on the method used to calculate the averages, the average SiC grain size had a large standard deviation. The SiC grain size also decreased with increasing SiC content, which is a somewhat surprising result. At this time, this result has not been studied in further detail. In the end, it can be concluded that the elastic modulus, hardness and flexure strength of ZrB_2–SiC materials increased with increasing SiC content. Part of the increase in elastic modulus, strength and hardness with increasing SiC content can be attributed to the reduction in porosity in the sintered ZrB_2–SiC ceramics with increasing SiC content. Even though various relationships[33–35] have been proposed for the effect of porosity on elastic modulus, flexure strength, and hardness, the general trend of these three mechanical properties is that the property values decrease with increasing porosity. As shown in Table 3, the sintered density of the ZrB_2–SiC ceramics increased with SiC content, i.e., the porosity decreased from ~3% for a SiC content of 10 vol% to less than 1% for a SiC content of 30 vol%. As a result, the modulus, strength, and hardness all increased with SiC contents. In addition to the effect of porosity, grain size also influences strength and hardness. As shown in Fig. 4, grain sizes of both ZrB_2 and SiC

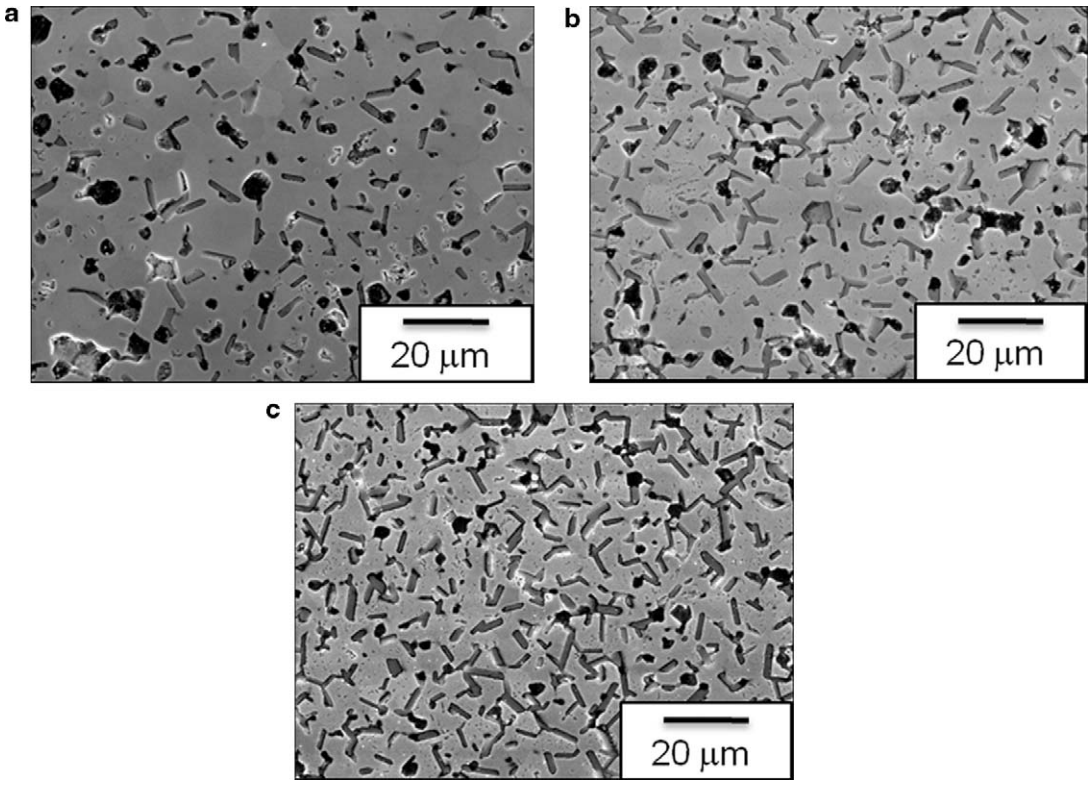

Fig. 3. Microstructure of ZrB_2 ceramics containing (A) 10 vol%, (B) 20 vol%, and (C) 30 vol% SiC (UF-25) additions and 5 wt% carbon.

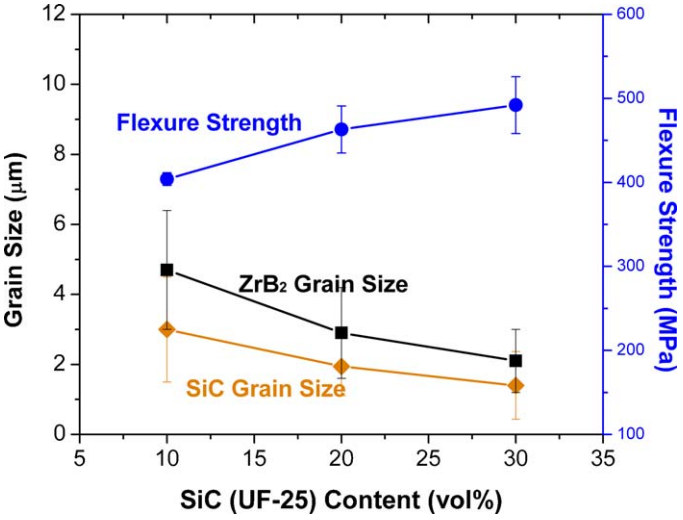

Fig. 4. Room temperature flexure strength, as well as ZrB_2 and SiC grain sizes, for ZrB_2–SiC materials as a function of SiC (UF-25) volume fraction.

in the sintered ZrB_2–SiC ceramics decreased with increasing SiC content. Therefore, the ZrB_2–30%SiC ceramics had the highest flexure strength of 492 MPa, compared to 404 MPa for ZrB_2–10% SiC. The effect of grain sizes on flexure strength will be discussed further in the next section. For hardness of the sintered ZrB_2–30%SiC ceramics, the smaller grain size resulted in ceramics with a higher density of grain boundaries. As a result, larger stresses were required to deform the finer grain size ceramics.[30,36] In addition to porosity and grain boundary effects, the higher inherent hardness of SiC (24.5–32 GPa),[37,38] compared to ZrB_2 (22.1–23 GPa),[21,39] also resulted in an increase in hardness with increasing SiC volume fraction. Based on the mechanical property results to this point, ZrB_2–30 vol% SiC with 5 wt% C was selected for additional studies on the effect of starting SiC particle size.

3.3. Effect of SiC particle size on the mechanical properties

The Griffith criterion predicts that the flexure strength of ceramic materials is inversely proportional to the square root of the critical flaw size. In the absence of other, larger flaws, strength is typically inversely proportional to the square root of the average grain size, i.e., a smaller grain size results in higher flexure strength. Further, previous analysis has concluded that it appears to be the SiC particle size that controls the strength of hot pressed ZrB_2–SiC materials.[30,40] For instance, strength values of <400 MPa were reported for ZrB_2–30% SiC hot-pressed at 1950°C producing an average SiC particle size of ~6 μm. Strengths over 900 MPa have only been reported for materials with SiC particles sizes of 1 μm or less. Based on these considerations the ZrB_2–30% SiC materials made using the finest SiC powder from this study should have the highest flexure strengths, compared to ZrB_2–30% SiC materials made using coarser powders.

In the present study, the ZrB_2 powder was attrition milled to reduce its average particle size from nominally 2 μm to ~0.6 μm prior to pressing. Specimens were prepared using milled ZrB_2 powder, 30 vol% of SiC powder having three different particle sizes (0.45 μm, 1.05 μm, or 1.45 μm), with 5 wt% carbon added to enhance densification. The specimens were then sintered at 1925 °C–2050 °C for 1.5 h. The densities of all of the ZrB_2–30% SiC materials in this part of the study were greater than 98% of their theoretical density.

The elastic modulus, hardness and fracture toughness of sintered ZrB_2–30 vol% SiC ceramics were comparable to hot pressed ZrB_2–SiC materials[21,25,29,40] (Table 4). In contrast to the previous studies, the ZrB_2–30% SiC material made using the finest SiC powder, which had a starting SiC particle size of 0.45 μm, had the lowest mean strength (~490 MPa). The ZrB_2–30% SiC material made using the mid-sized SiC powder, with a starting particle size of 1.05 μm, had the highest mean strength (~600 MPa), while the coarsest powder (1.45 μm starting particle size) resulted in a mean strength of ~560 MPa. To explain the variations in flexural strengths, in particular as to why the finest SiC raw powder resulted in the lowest flexure strength, the microstructures of the three materials were analyzed. Fig. 5 compares the microstructures of ZrB_2–30% SiC fabricated from the three different SiC powders. SEM analysis revealed that the SiC grains in the ceramics prepared using the finest powder (Figs. 5(c)) were predominantly elongated with a whisker-like morphology. The other two ceramics (Figs. 5(a) and (b), respectively) had microstructures with an equiaxed SiC grain morphology. The elongation of the SiC particles was evaluated by calculating the aspect ratio of the SiC grains for each material. The SiC grains for the largest starting particle size (1.5 μm) were equiaxed with an aspect ratio of 1.05. The aspect ratio increased to ~4.25 when the finest SiC powder (starting particle size of 0.45 μm) was used. As discussed above, it appears that the SiC particles form a percolating network when the finest particle size is used, but do not form a continuous network for the other two starting powders.[41,42]

Based on the microstructures, the lower flexure strength of the ZrB_2–30 vol% SiC made using the finest starting SiC powder can be attributed to the formation of elongated SiC grains. The average length of the SiC grains in the composition prepared from the finest SiC powder was 13 μm compared to average SiC grain diameters in the range of 2.0–2.5 μm for the other SiC powders. If the size of SiC grains controls the strength, as discussed earlier, then the material with elongated SiC grains would be expected to have the lowest strength.

As has been discussed by Zimmermann et al.,[43] it is the difference in the coefficient of thermal expansion between SiC (4.5×10^{-6}/°C) and ZrB_2 (6.8×10^{-6}/°C) that leads to a residual tensile stress state in the ZrB_2 matrix and which adversely affects the flexure strength for ZrB_2–30% SiC materials. This effect would be expected to be pronounced for elongated SiC grains, due to the development of a larger volume of tensile residual stresses in the ZrB_2 matrix during cooling from the processing temperature. Upon cooling from the sintering temperatures, the SiC grains will not contract as quickly as the ZrB_2 matrix, resulting in a tensile residual stress in the ZrB_2 matrix in proximity to the dispersed SiC particles.[43] Watts et al. have recently reported the tensile stresses in the ZrB_2 matrix to be

Table 4
Effect of initial SiC particle size on the ZrB_2 and SiC grain sizes in the final microstructure and properties of sintered ZrB_2–30% SiC.

SiC Grade	UF-25	UF-10	UF-5	UF-5
SiC particle size	0.45 μm	1.05 μm	1.45 μm	1.45 μm
ZrB_2	Milled	Milled	Milled	As-received
ZrB_2 particle size	0.6 μm	0.6 μm	0.6 μm	1.45 μm
Sintered Density	99%	99%	99%	99%
SiC grain size	$13 \pm 1.9 \times 2 \pm 0.2$ μm	2.0 ± 0.8 μm	2.4 ± 0.9 μm	2.5 ± 0.8 μm
ZrB_2 grain size	2.6 ± 0.8 μm	2.8 ± 1.4 μm	4.0 ± 1.8 μm	5.5 ± 2.2 μm
E (GPa)	490 ± 7	511 ± 7	497 ± 7	499 ± 7
K_{1C} (MPa $m^{1/2}$)	3.5 ± 0.3	3.8 ± 0.2	4.1 ± 0.3	4.2 ± 0.2
σ (MPa)	492 ± 71	604 ± 69	559 ± 82	537 ± 54

~800 MPa using Raman spectroscopy and neutron diffraction methods.[44] In addition, the tensile stress decreases with the distance from the interface between the ZrB_2 matrix and the SiC particulate phase. Thus, the distribution of the tensile stresses in the matrix (ZrB_2) can be computed as a function of the distance (r) from the interface according to the Eshelby equation (1).[45] The results of this calculation are shown in Fig. 6. As seen from the graph, the tensile stress drops more rapidly with distance when the SiC grains (having average size d) become smaller. For example, the tensile stress is only 30% of the maximum stress at the interface at a distance of 1 μm from the interface at a SiC particle size of 2 μm. In contrast, 85% of the maximum stress is retained at the same distance from the interface when the SiC particle size is 15 μm. As a result, a higher volume fraction of the ZrB_2 matrix is under a stress state that is near the applied tensile stress when the dispersed SiC particles are larger.

Microstructure analysis results for the three ZrB_2–30% SiC compositions, summarized in Table 4, reveal that using the SiC powder with the finest starting particle size resulted in the formation of elongated SiC particles in the final ceramic. For ZrB_2–30 vol% SiC sintered at 1950 °C, the average length of the SiC particles was 13 μm. Considering the average size of the ZrB_2 grains in the ZrB_2–30% SiC composite prepared from the finest SiC powder (UF-25) was ~3 μm (Table 4), and they were surrounded by elongated SiC particles, it can be concluded that all of ZrB_2 grains were under a tensile stress of nominally 70% of the maximum applied tensile stress. In contrast, only 10% of the maximum applied tensile stress was present at the center of the ZrB_2 grains for the ZrB_2–30% SiC (UF-10) com-

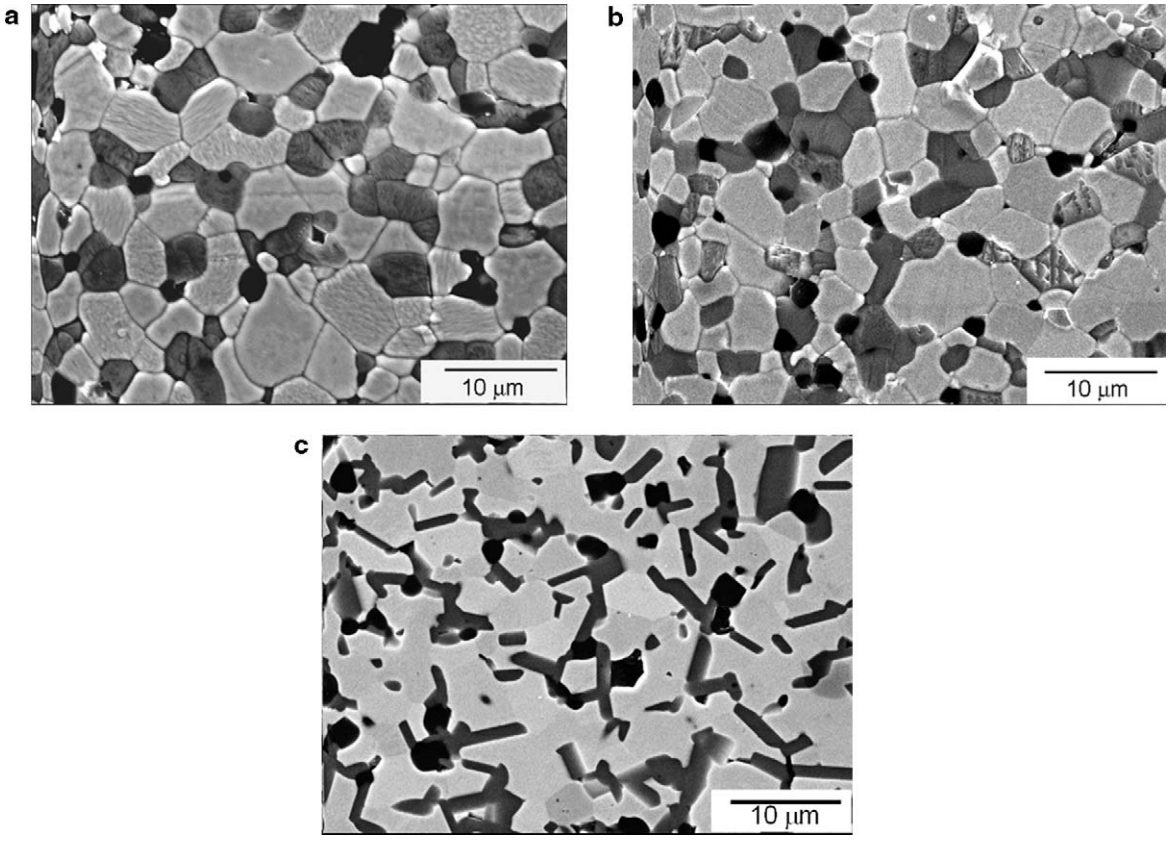

Fig. 5. Microstructures of ZrB_2–30 vol% SiC with SiC powders with starting particle sizes of (a) 1.45 μm, (b) 1.05 μm, and (c) 0.45 μm.

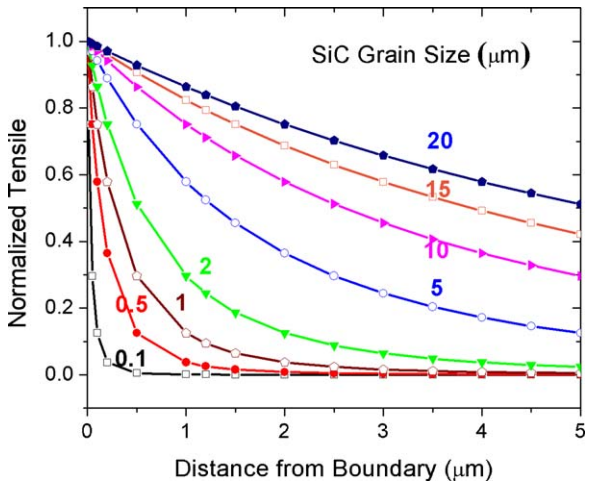

Fig. 6. Tensile stress distribution, based on an Eshelby type analysis, in ZrB_2 grains in ZrB_2–30% SiC composites with various SiC particle sizes.

posite that had equiaxed SiC grains. Therefore, the larger ZrB_2 volume fraction under a tensile residual stress in the ZrB_2–30% SiC composite with elongated grains resulted in an increased flaw size, which reduced strength.

$$2\sigma_{ZrB_2} = \frac{\left(\alpha_{ZrB_2} - \alpha_{SiC}\right)\Delta T}{(1-2\upsilon ZrB_2)/2EZrB_2 + (1-2\upsilon_{SiC})/E_{SiC}}\left(\frac{d}{r+d}\right)^3 \quad (1)$$

4. Concluding remarks

The effect of starting SiC particle size on the flexure strength of pressurelessly sintered ZrB_2–SiC ceramics was investigated. Zirconium diboride (ZrB_2) ceramics containing 10, 20 and 30 vol% silicon carbide (SiC) were sintered to near full density at temperatures as low as 1875 °C with the addition of 4 wt% B_4C based on the amount of ZrB_2 and 5 wt% C based on the amount of SiC. The results revealed that the material prepared using a 5 wt% C addition and SiC powder with an initial particle size of 1.05 μm had higher room temperature flexure strengths, around 600 MPa, compared to ZrB_2–SiC prepared from SiC with either finer (initial particle size of 0.45 μm) or larger (initial particle size of 1.45 μm) starting particle sizes.

The following conclusions were drawn from the results of the research:

(1) A minimum carbon addition of 2.8 wt% based on the SiC weight in the batch was calculated to be enough to react with and remove the SiO_2 from the SiC particle surfaces. However, experiments showed that this amount was insufficient and resulted in incomplete densification of ZrB_2–SiC. Carbon additions of 10 wt% based on the SiC weight resulted in the formation of excess carbon in the microstructure, which reduced the strength of the resulting ceramics. Either insufficient densification or excess carbon resulted in lower strengths for sintered ZrB_2–SiC. A carbon addition of 5 wt% based on the SiC content could be sintered to near full density and resulted in the highest strength.

(2) The strength of hot-pressed ZrB_2–SiC increased with decreasing starting SiC particle size. However, using the SiC powder with the finest starting particle size (0.45 μm) did not result in the highest flexure strength for pressureless sintered ZrB_2–SiC ceramics due to elongation of SiC grains during sintering with longer time, compared to hot-pressing. The elongated SiC grains, and the mismatch in thermal expansion coefficient between ZrB_2 and SiC, resulted in larger tensile stresses in the ZrB_2 grains. Based on an average ZrB_2 grain size of 3.0 μm, the tensile stresses at the grain centers were calculated to be approximately 70% of the maximum tensile stress at the ZrB_2–SiC interface for elongated grains compared to only ~10% of the maximum tensile stress for equiaxed SiC grains. Consequently, the residual stress lowered the flexure strength of the ZrB_2–SiC ceramics.

(3) Using the SiC powder with the middle starting particle size (1.05 μm) resulted in an equiaxed SiC grain morphology and the smallest ZrB_2 and SiC grains. As a result, ceramics prepared from this starting powder had the highest flexure strength (600 MPa) compared with ceramics prepared from finer or coarser SiC powders.

References

[1]. Gasch MJ, Ellerby DT, Johnson SM. Ultra high temperature ceramic composites. In: Bansal NP, editor. *Handbook of ceramic composites*. Boston: Kluwer Academic Publishers; 2005. p. 197–224.
[2]. Fahrenholtz WG, Hilmas GE, Talmy IG, Zaykoski JA. Refractory diborides of zirconium and hafnium. *J Am Ceram Soc* 2007;**90**(5):1347–64.
[3]. Telle R, Sigl LS, Takagi K. Boride-based hard materials. In: Riedel R, editor. *Handbook of Ceramic Hard Materials*. Weinheim, Germany: Wiley-VCH; 2000. p. 802–945.
[4]. Cutler RA. Engineering properties of borides. In: Schneider Jr SJ, editor. *Ceramics and glasses: engineered materials handbook*, vol. 4. Materials Park, OH: ASM International; 1991. p. 787–803.
[5]. Levine SR, Opila EJ, Halbig MC, Kiser JD, Singh M, Salem JA. Evaluation of ultra-high temperature ceramics for aeropropulsion use. *J Eur Ceram Soc* 2002;**22**(14–15):2757–67.
[6]. Shaffer PTB. An oxidation resistant boride composition. *Am Ceram Bull* 1962;**41**(2):96–9.
[7]. Fahrenholtz WG. The ZrB_2 volatility diagram. *J Am Ceram Soc* 2005;**88**(12):3509–12.
[8]. Tripp WC, Davis HH, Graham HC. Effect of an SiC addition on the oxidation of ZrB_2. *Am Ceram Bull* 1973;**52**(8):612–6.
[9]. Rezaie A, Fahrenholtz WG, Hilmas GE. Evolution of structure during the oxidation of zirconium diboride-silicon carbide in air up to 1500 °C. *J Eur Ceram Soc* 2007;**27**(6):2495–501.
[10]. Li J, Lenosky TJ. Thermochemical and mechanical stabilities of the oxide scale of ZrB_2 + SiC and oxygen transport mechanisms. *J Am Ceram Soc* 2008;**91**(5):1475–80.
[11]. Clougherty EV, Pober RL, Kaufman L. Synthesis of oxidation resistant metal diboride composites. *Trans Metall Soc AIME* 1968;**242**(6):1077–82.
[12]. Bongiorno A, Först CJ, Kalia RK, Li J, Marschall J, Nakano A, et al. A perspective on modeling materials in extreme environments: oxidation of ultrahigh-temperature ceramics. *MRS Bull* 2006;**31**(5):410–8.
[13]. Fahrenholtz WG. Thermodynamic analysis of ZrB_2–SiC oxidation: formation of a SiC-depleted region. *J Am Ceram Soc* 2007;**90**(1):143–8.
[14]. Opeka MM, Talmy IG, Zaykoski JA. Oxidation-based materials selection for 2000 °C+ hypersonic aerosurfaces: theoretical considerations and historical experience. *J Mater Sci* 2004;**39**(19):5887–904.
[15]. Monteverde F, Bellosi A. Oxidation of ZrB_2-based ceramics in dry air. *J Electrochem Soc* 2003;**150**(11):B552–9.

[16]. Wang CR, Yang JM, Hoffman W. Thermal stability of refractory carbide/boride composites. *Mater Chem Phys* 2002;**74**(3):272–81.
[17]. Karlsdottir SN, Halloran JW. Rapid oxidation characterization of ultra-high temperature ceramics. *J Am Ceram Soc* 2007;**90**(10):3233–8.
[18]. Sciti D, Brach M, Bellosi A. Long-term oxidation behavior and mechanical strength degradation of a pressureless sintered ZrB_2–$MoSi_2$ ceramic. *Scripta Mater* 2005;**53**:1297–302.
[19]. Opila E, Levine S, Lorincz J. Oxidation of ZrB_2- and HfB_2-based ultra-high temperature ceramics: effect of Ta additions. *J Mater Sci* 2004;**39**(19):5969–77.
[20]. Talmy IG, Zaykoski JA, Opeka MM, Smith AH. Properties of ceramics in the system ZrB_2–Ta_5Si_3. *J Mater Res* 2006;**21**(10):2593–9.
[21]. Chamberlain AL, Fahrenholtz WG, Hilmas GE. High-strength zirconium diboride-based ceramics. *J Am Ceram Soc* 2004;**87**(6):1170–2.
[22]. Monteverde F, Melandri C, Gicciardi S. Microstructure and mechanical properties of HfB_2 + 30 vol% SiC composite consolidated by spark plasma sintering. *Mater Chem Phys* 2006;**100**(2–3):513–9.
[23]. Monteverde F. Beneficial effects of an ultra-fine α-SiC incorporation on the sinterability and mechanical properties of ZrB_2. *Appl Phys* 2006;**A82**:329–37.
[24]. Hwang SS, Vasiliev AL, Padture NP. Improved processing and oxidation-resistance of ZrB_2 ultra-high temperature ceramics containing SiC nanodispersoids. *Mater Sci Eng A* 2007;**464**:214–6.
[25]. Zimmermann JW, Hilmas GE, Fahrenholtz WG, Monteverde F, Bellosi A. Fabrication and properties of reactive hot-pressed ZrB_2–SiC ceramics. *J Eur Ceram Soc* 2006;**27**:2729–36.
[26]. Zhang SC, Hilmas GE, Fahrenholtz WG. Pressureless densification of zirconium diboride with boron carbide additions. *J Am Ceram Soc* 2006;**89**(5):1544–50.
[27]. Zhang H, Yan Y, Huang Z, Liu X, Jiang D. Properties of ZrB_2–SiC ceramics by pressureless sintering. *J Am Ceram Soc* 2009;**92**(7):1599–602.
[28]. Monteverde F, Guicciardi S, Bellosi A. Advances in microstructure and mechanical properties of zirconium diboride based ceramics. *Mater Sci Eng* 2003;**346**:310–9.
[29]. Monteverde F, Bellosi A. Development and characterization of metal-diboride-based composites toughen with ultra-fine SiC particulates. *Solid State Sci* 2005;**7**:622–30.
[30]. Zhu SM, Fahrenholtz WG, Hilmas GE. Influence of silicon carbide particle size on the microstructure and mechanical properties of zirconium diboride-silicon carbide ceramics. *J Eur Ceram Soc* 2007;**27**: 2077–83.
[31]. Zhang XH, Luo XG, Han JC, Li JP, Han WB. Electronic structure, elasticity and hardness of diborides of zirconium and hafnium: first principles calculations. *Comput Mater Sci* 2008;**44**:411–21.
[32]. Munro RG. Material properties of a sintered alpha-SiC. *J Phys Chem Ref Data* 1997;**26**(5):1195–203.
[33]. Kingery WR, Bowen HK, Uhlmann DR. *Introduction to ceramics*. New York: John Wiley & Sons; 1975. p. 775.
[34]. Jian-Feng Yang, Tatsuki Ohji, Shuzo Kanzaki. Microstructure and mechanical properties of silicon nitride ceramics with controlled porosity. *J Am Ceram Soc* 2002;**85**(6):1512–6.
[35]. Nielsen LF. Elasticity and damping of porous materials and impregnated materials. *J Am Ceram Soc* 1984;**67**(2):93–8.
[36]. Lee H, Speyer RF. Hardness and fracture toughness of pressurelesss intered boron carbide (B_4C). *J Am Ceram Soc* 2002;**85**(5):1291–3.
[37]. Munro RG. Material properties of a sintered α-SiC. *J Phys Chem Ref Data* 1997;**26**(5):1195–203 [published by American Chemical Society].
[38]. Quinn JB, Quinn GD. Indentation brittleness of ceramics: a fresh approach. *J Mater Sci* 1997;**32**:4331–46 [published by Chapman and Hall].
[39]. Cutler RA. Engineering properties of borides. In: Schneider Jr SJ, editor. *Engineered materials handbook*, vol. 4. ASM International; 1991. p. 787–803.
[40]. Rezaie A, Fahrenholtz WG, Hilmas GE. Effect of hot pressing time and temperature on the microstructure and mechanical properties of ZrB_2–SiC. *J Mater Sci* 2007;**42**(8):2735–44.
[41]. Kusy RP. Influence of particle size ratio on the continuity of aggregates. *J Appl Phys* 1977;**48**(12):5301–5.
[42]. Malliaris A, Tuener DT. Influence of particle size on the electrical resistivity of compacted mixtures of polymeric and metallic powders. *J Appl Phys* 1971;**42**(2):614–8.
[43]. Zimmermann JW, Hilmas GE, Fahrenholtz WG. Thermal shock resistance of ZrB_2 and ZrB_2–30% SiC. *Mater Chem Phys* 2008;**112**: 140–5.
[44]. Watts J, Hilmas GE, Fahrenholtz WG. Stress measurements in ZrB_2–SiC composites using Raman spectroscopy and neutron diffraction. *J Eur Ceram Soc* 2010;**30**(11):2165–71.
[45]. Barsoum M. *Fundamentals of ceramics*. New York: McGraw-Hill Companies, Inc.; 1997.